Available online at www.sciencedirect.com
SCIENCE DIRECT®
Catalysis Today 96 (2004) 147–153
CATALYSIS TODAY
www.elsevier.com/locate/cattod

Isomerisation of α-pinene oxide over B_2O_3/SiO_2 and Al-MSU catalysts

D.B. Ravindra, Y.T. Nie, S. Jaenicke, G.K. Chuah*

Department of Chemistry, National University of Singapore, Kent Ridge, Singapore 119260, Singapore

Available online 24 August 2004

Abstract

The isomerisation of α-pinene oxide to campholenic aldehyde was investigated over a number of solid acids—B_2O_3/SiO_2, $ZnCl_2$/MCM-41, Al-MCM-41, HY zeolites and Al-MSU-S_{FAU}. Irrespective of the loading, the selectivity to campholenic aldehyde over B_2O_3/SiO_2 was ∼69% at 25 °C. The initial rate for the isomerisation of α-pinene oxide was a maximum at 15 wt.% B_2O_3 loading. Both Lewis and Brønsted acid sites were present in B_2O_3/SiO_2 samples although at higher loadings of B_2O_3, Brønsted acidity predominated. Under anhydrous conditions, no crystalline phases of boron oxide were detected up to a B_2O_3 loading of 20 wt.%, but upon exposure to ambient environment, boric acid was formed. The Lewis acid, $ZnCl_2$/MCM-41, was not very active but highly selective (85%) for campholenic aldehyde. Al-MCM-41 and HY zeolites showed high conversion but the selectivity was dependent on the Al content, varying from 49 to 66%. By incorporating both microporosity and mesoporosity in mesostructured Al-MSU-S_{FAU} (Si/Al 70), good activity and selectivity to campholenic aldehyde, 86%, was observed.

Keywords: Isomerisation; α-Pinene oxide; Campholenic aldehyde; Micro-/mesoporosity; Solid acids

1. Introduction

Campholenic aldehyde is used in the fragrance industry for its sandalwood scent. Of the two isomers, the (1′R)-(+)-campholenic aldehyde has the intensive green grass-like spicy scent while the (1′S)-(−) isomer does not have a perceptible odour. The isomerisation of α-pinene oxide results in campholenic aldehyde, along with many other isomers such as *trans*-carveol, *trans*-sobrerol, isopinocamphone and *p*-cymene (Scheme 1). The reaction is catalysed by acidic sites with Lewis acidity favouring the formation of campholenic aldehyde and Brønsted acidity resulting in isomerisation products such as *trans*-carveol, *trans*-sobrerol and *p*-cymene. The maximum selectivity to campholenic aldehyde over Brønsted acids is 55% while Lewis acids such as Zn halides give selectivities up to 85% [1]. However, the use of $ZnCl_2$ or $ZnBr_2$ as homogeneous catalysts has several disadvantages such as lack of regeneration, corrosion problems, toxicity and waste water pollution. A number of heterogeneous catalysts for the reaction have been reported. Hölderich et al. [1] found that HCl-treated H-USY zeolite was particularly active. At 25 °C, the selectivity to campholenic aldehyde was 70% but by carrying out the reaction at −30 °C, the selectivity improved to ∼80%. The active sites were proposed to be highly dispersed Lewis acidic species (extraframework aluminium) within the zeolitic framework, although the participation of some Brønsted acid sites could not be excluded. The acid treatment of H-USY removed amorphous silica species which covered the active sites, and created additional mesoporosity. Silica-supported zinc triflate (trifluoromethanesulfonate) was also reported as showing high activity [2]. In comparison, the pure triflate was less active due to poorer dispersion. The silica-supported zinc triflate had predominantly Lewis acid sites with some Brønsted acidity which was attributed to the interaction of the triflate groups with the hydroxyl groups on silica. The selectivity was in the range of 55–76% at a reaction temperature of 85 °C. Kunkeler et al. [3] found that zeolite titanium beta was a very good catalyst for the reaction with a selectivity

* Corresponding author. Tel.: +65 6874 2839; fax: +65 6779 1691.
E-mail address: chmcgk@nus.edu.sg (G.K. Chuah).

0920-5861/$ – see front matter © 2004 Elsevier B.V. All rights reserved.
doi:10.1016/j.cattod.2004.06.117

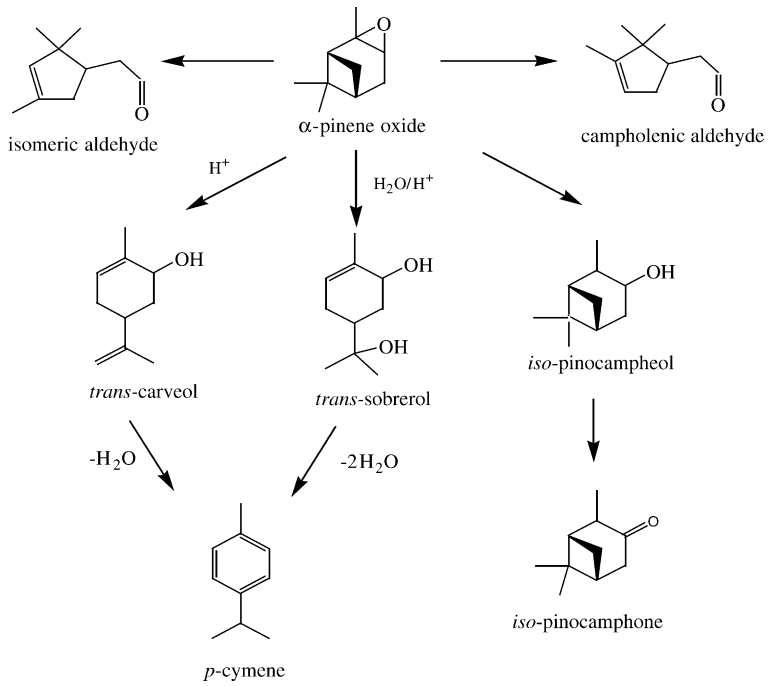

Scheme 1. Major products formed during acid-catalyzed rearrangement of α-pinene oxide.

of ~89% at 7% conversion in the liquid phase. The selectivity decreased when polar solvents were used. The high selectivity to campholenic aldehyde observed in nonpolar solvents was attributed to a preferential adsorption of the nonpolar solvent by the hydrophobic Ti-Beta, so that the concentration of α-pinene oxide at the active sites is low. Hölderich et al. [1] reported that the suitability of USY zeolite as catalyst for the isomerisation of α-pinene oxide depended on its three-dimensional large pore system of 0.74 nm with supercages of 1.2 nm and a large amount of mesopores. Such a pore structure allowed good migration of the reactant into the channel system.

In this study, we investigate the use of silica-supported boron oxide in the isomerisation of α-pinene oxide and compare its activity with a number of solid acids. Boron oxide is a Lewis acid with the electron deficient boron acting as an electron acceptor. Hence, it coordinates even weak bases to form four-coordinate borate species. When supported on oxides such as alumina, silica, titania or zirconia, a strong solid acid is obtained [4,5]. The boron exists as BO_3 and BO_4 species and the Brønsted acidity has been correlated to the BO_4 species [6].

Al-MSU-S_{FAU} was synthesized from nanoclustered zeolite seeds as framework precursors [7]. After addition of a micellar template, the zeolite seeds assemble into an ordered mesostructure around the templating structure. Hence, a mesoporous structure with the walls having microporosity is achieved. The incorporation of tetrahedrally coordinated Al leads to Brønsted acidity. Such MSU materials have been reported to show a higher degree of acidity and hydrothermal stability than conventional Al-MCM-41 [8–10].

2. Experimental

2.1. Catalyst preparation

The appropriate weight of boric acid (Riedel-deHaen) to give 5, 10, 15 and 20 wt.% boron oxide loading was dissolved in warm deionized water and added to the SiO_2 60 (Merck). After stirring gently for 2 h, the excess water was evaporated, and the slurry was dried overnight at 120 °C. The catalysts were calcined at 350 °C for 8 h in air.

$ZnCl_2$ supported on MCM-41 containing 2, 4 and 8 mmol $ZnCl_2$/g were prepared by impregnating siliceous MCM-41 with an ethanolic solution of $ZnCl_2$. The solvent was removed using a rotary evaporator and the sample was dried under vacuum at 120 °C for 4 h [11]. Al-MCM-41 with Si/Al 70 was prepared following Ref. [12].

Al-MSU-S_{FAU} material with Si/Al 70 was prepared following Ref. [13]. An alumino–silicate gel was formed by dissolving NaOH, $NaAlO_2$ and sodium silicate solution in water. This gel was stirred at room temperature for 1 h, then heated under reflux with moderate stirring at 100 °C overnight to form the zeolite Y seed solution. The seed solution was added to a solution of cetyltrimethyl ammonium bromide (CTAB) at room temperature and the pH was lowered to about pH 9 by addition of dilute sulfuric acid. The final gel composition can be represented as 0.09 NaOH:0.90 Na_2SiO_3:0.0128 $NaAlO_2$:0.20 CTAB:0.65 H_2SO_4:100 H_2O. The gel was aged at RT for 1 h and then kept at 100 °C for 48 h in a Teflon-lined autoclave under static conditions. The solid was recovered by filtration and calcined at 540 °C for 12 h to remove the template, ion ex-

changed with NH_4NO_3 solution, and recalcined to obtain the H^+ form. HY zeolites with Si/Al 10.4, 24 and 60 were obtained from Zeolyst International.

2.2. Catalyst characterisation

The surface area and pore volumes were measured by nitrogen adsorption (Quantachrome Nova 2000). The samples were dried at 300 °C prior to measurements. The crystal phase was determined using a Siemens D5005 powder X-ray diffractometer equipped with Cu anode, and variable primary and secondary beam slits. Variable temperature XRD was carried out using an in situ cell attached to a Bruker D8 diffractometer. The acidity of the samples was determined by IR of pyridine adsorbed onto self-supporting wafers (8–10 mg). The sample was mounted in an evacuable Pyrex IR cell with NaCl windows. A Bio-Rad FTS 165 FT-IR spectrometer was used with a resolution of 4 cm^{-1}. The sample was dried by evacuating under vacuum (10^{-3} mbar) for 2 h at 300 °C and cooled down to room temperature. Pyridine was introduced into the sample cell at a pressure of 22 mbar for 15 min, followed by evacuation for an hour. The FT-IR spectrum of adsorbed pyridine was measured at room temperature. Successive heating to 100 and 200 °C for 1 h resulted in the desorption of H-bonded and weakly bonded pyridine.

Solid state NMR spectra were taken of the samples using a Bruker DRX-400 NMR spectrometer. The ^{11}B-MAS spectra were recorded at 128.4 MHz using 8° rf pulses, 1 s recycle delay and a spinning rate of 12 kHz. The chemical shift was referenced to BF_3 etherate. The spectra were background subtracted for boron nitride in the zirconia rotor. The ^{27}Al-MAS NMR spectra were obtained at 104.26 MHz with an excitation pulse of 1.7 μs and a recycle delay of 5 s. The spectra were referenced to aqueous $Al(NO_3)_3$. The ^{29}Si-MAS NMR spectra were recorded at 79.5 MHz using 3.0 μs pulse with a recycle delay of 20 s. The chemical shifts were measured relative to sodium 3-(trimethylsilyl)-1-propanesulfonate.

2.3. Catalytic reaction

1.5 g of α-pinene oxide (Aldrich, purity 97%) and 6 g of toluene were placed into a round bottomed flask equipped with guard tube. The catalyst (0.15 g) was first dried at 100 °C before adding to the reaction mixture. The suspension was agitated with a magnetic stirrer and the reaction temperature was varied from 0 to 50 °C. Aliquots were withdrawn at regular intervals and analyzed by gas chromatography (Agilent 6890, HP 5 column). The products were identified by verification with authentic samples and by GC-MS (Shimadzu GCMS-QP5000, DB5MS column). The starting material was only 97% pure and contained a small amount of campholenic aldehyde together with α-pinene oxide. This was taken into account when calculating the conversion and selectivity.

Table 1
Textural properties of supported catalysts

Catalyst	Surface area ($m^2\ g^{-1}$)	Pore volume ($cm^3\ g^{-1}$)
SiO_2	288	0.75
5% B_2O_3/SiO_2	276	0.70
10% B_2O_3/SiO_2	255	0.63
15% B_2O_3/SiO_2	235	0.57
20% B_2O_3/SiO_2	231	0.52
$ZnCl_2$/MCM-41 (2 mmol g^{-1})	767	0.60
$ZnCl_2$/MCM-41 (4 mmol g^{-1})	690	0.58
$ZnCl_2$/MCM-41 (8 mmol g^{-1})	413	0.28
Al-MCM-41 (Si/Al 70)	682	0.78
Al-MSU-S (Si/Al 70)	976	0.95
HY (Si/Al 10.4)	750	–
HY (Si/Al 24)	730	–
HY (Si/Al 60)	780	–

3. Results and discussion

3.1. Textural properties of catalysts

An increase in boron oxide loading resulted in a decrease of surface area and pore volume (Table 1). The surface area decreased from 288 $m^2\ g^{-1}$ in SiO_2 to 231 $m^2\ g^{-1}$ in the sample with 20 wt.% B_2O_3 loading. The pore volume decreased from 0.75 to 0.52 $cm^3\ g^{-1}$. The pore size distribution curves narrowed with loading and showed a shift to a smaller mean pore diameter, indicating a uniform coverage of the support rather than clogging of pore entrances. The XRD patterns of B_2O_3/SiO_2 were largely amorphous with only a few sharp lines (Fig. 1). The most intense peak was observed at $2\theta = 28°$ for all the B_2O_3/SiO_2 catalysts. The intensity of this peak increased with the increase of boron oxide loading. Except for 5% B_2O_3/SiO_2, all the other boron oxide-loaded

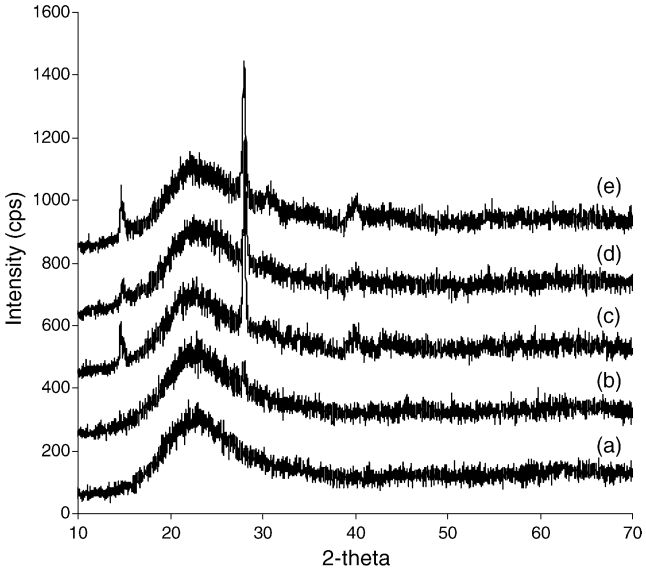

Fig. 1. XRD patterns of (a) SiO_2 and B_2O_3/SiO_2 (wt.%) catalysts with (b) 5% B_2O_3, (c) 10% B_2O_3, (d) 15% B_2O_3, (e) 20% B_2O_3 measured at 25 °C.

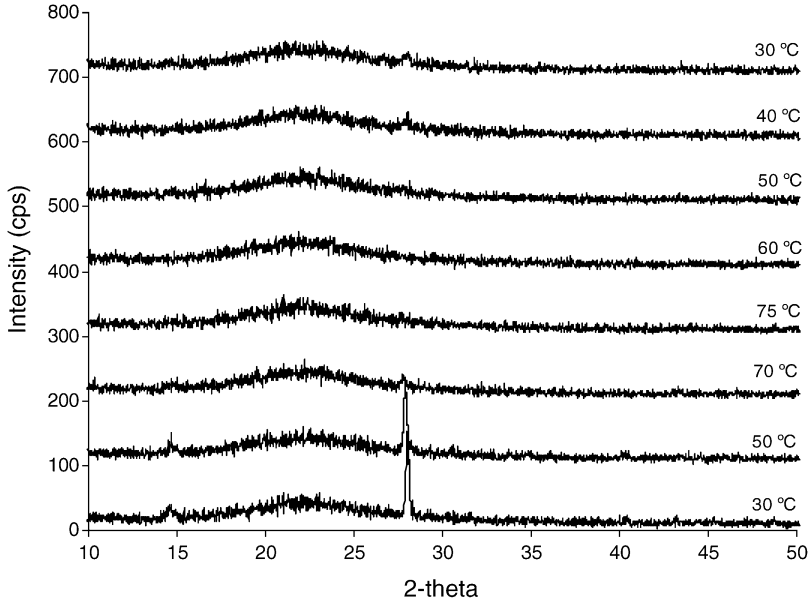

Fig. 2. XRD of 15 wt.% B_2O_3/SiO_2 as a function of temperature when heated in an in situ temperature cell.

catalysts showed additional peaks of lower intensity at $2\theta = 15^\circ$, 31° and 40°. Comparing with the PDF library for X-ray diffraction patterns, these peaks could be due to either B_2O_3 or H_3BO_3. By heating a 15 wt.% B_2O_3/SiO_2 sample in an in situ heating chamber, the intensity of the peaks continuously decreased with temperature up to 70–75 °C (Fig. 2). On cooling down in the static air environment, no peaks were observed. However, after exposure to the environment for a few minutes, the peaks at $2\theta = 15^\circ$ and 28° could once again be observed. This shows that in the crystalline phase, the boron oxide is present in the hydrated form as boric acid.

Fig. 3 shows the ^{11}B-MAS NMR spectra of B_2O_3/SiO_2 catalysts with different boron oxide loading. In amorphous and crystalline compounds, boron may exist in tetrahedral [BO_4] units and trigonal [BO_3] units. The tetrahedrally coordinated boron could arise from the coordination of hydroxyl groups to [BO_3] units or from the coordination of oxygen from the support to the three-coordinated boron [14]. The spectra of the five compounds showed peaks corresponding to [BO_3] and [BO_4] units. The signal corresponding to [BO_4] unit is around 5 ppm. The signal for trigonally coordinated [BO_3] was split and broadened due to a second-order quadrupolar effect [4]. With increase of boron oxide loading, the signal of [BO_4] became stronger and broader. After drying the 15% B_2O_3/SiO_2 for 48 h at 100 °C, the resonance due to tetrahedrally coordinated B was reduced compared to the three-coordinated boron. This supports the suggestion that part of the [BO_4] resonance is due to hydroxylated B species.

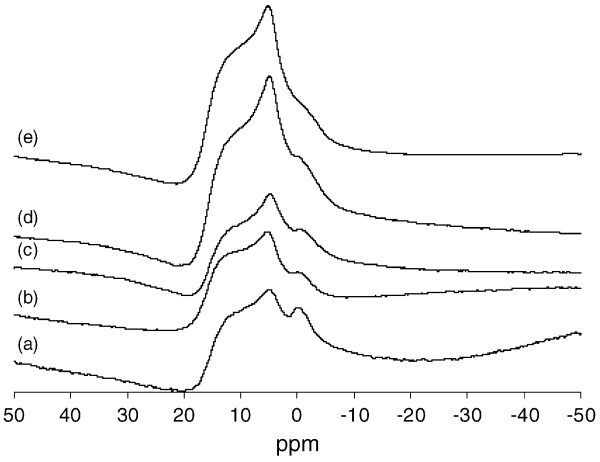

Fig. 3. ^{11}B-MAS NMR of (a) 5% B_2O_3, (b) 10% B_2O_3, (c) 15% B_2O_3, (d) 20% B_2O_3 and (e) 40% B_2O_3.

Al-MSU-S (Si/Al 70) had a surface area of 976 $m^2\,g^{-1}$ with a pore volume of 0.95 $cm^3\,g^{-1}$. The N_2 sorption isotherm was type IV with rectangular type H4 hysteresis loop at $P/P_0 > 0.4$ and capillary condensation steps at P/P_0 of 0.2–0.35. At the low pressure end, *t*-plot analysis showed that the sample had a very small amount of microporosity, 0.03 $cm^3\,g^{-1}$. The ^{27}Al-MAS NMR spectra of calcined Al-MSU-S sample showed a very strong and broad resonance centered around 53–55 ppm and a weak peak around 0 ppm. The 55 ppm signal was assigned to $Al(O)_4$ joined to four $Si(O)_4$ units in highly symmetrical tetrahedral coordination [8]. The peak at ~0 ppm was assigned to $Al(O)_6$ species in poorly symmetrical octahedral coordination.

3.2. IR pyridine adsorption

The infrared spectrum of pyridine adsorption at room temperature on SiO_2 shows bands at ~1446 and 1580 cm^{-1} due to hydrogen bonded pyridine (Fig. 4). A small band at ~1462 cm^{-1} is due to the pyridine adsorption at Lewis acid sites [15,16]. The low intensity of this band shows the

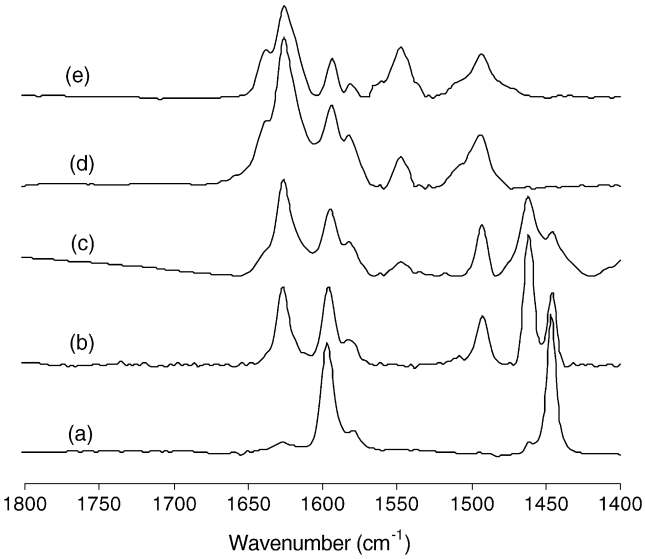

Fig. 4. IR spectra of pyridine adsorbed at room temperature on (a) SiO_2, (b) 5% B_2O_3/SiO_2, (c) 10% B_2O_3/SiO_2, (d) 15% B_2O_3/SiO_2 and (e) 20% B_2O_3/SiO_2.

weak Lewis acidity of the SiO_2 support. After impregnation of SiO_2 with 5 wt.% B_2O_3, the 1462 cm^{-1} band became more intense. In addition, bands at 1495 and 1626 cm^{-1} appeared. Both bands are due to coordinatively bonded pyridine at Lewis acid sites. Brønsted acidity was not noted in this sample. Brønsted acidity was observed from samples with 10 wt.% B_2O_3 and higher. Interestingly, with high B_2O_3 loading, the band at ~1462 cm^{-1} completely disappeared. However, the presence of bands at 1595 and 1626 cm^{-1} showed that Lewis acid sites were still present. On heating to 100 °C, the intensity of the bands decreased. The bands also narrowed as only stronger bound pyridine remained. Even after heating to 200 °C, some signal was still present, indicating that some very strong Lewis and Brønsted acid sites were present in these samples.

Since boron is a very small ion, it is envisaged that its role as a Lewis acid site may be limited in the presence of large oxygen ions. Hence, we postulate that the active Lewis acid sites are located at Si atoms. The presence of the electron deficient boron increases the Lewis acidity of the Si due to an inductive effect. As the loading of boron oxide increases, the entire silica surface is finally covered by an overlayer. At 20 wt.% boron loading, the band at 1462 cm^{-1} was no longer observed. From the surface area of silica, 288 m^2g^{-1}, and estimating a surface hydroxyl density of 5×10^{19} m^{-2}, a monolayer of boron oxide is expected to form at 12.5 wt.%. At 20 wt.% B_2O_3, the boron oxide should completely cover the surface so that no free Si sites are exposed. Whereas the concentration of Lewis acid sites went through a maximum, the concentration of Brønsted acid sites increased with boron oxide loading up to monolayer coverage as these sites are generated upon hydration of boron oxide.

In contrast to the B_2O_3/SiO_2 samples, Al-MSU-S had mainly Lewis acidity. The IR spectrum was very similar to

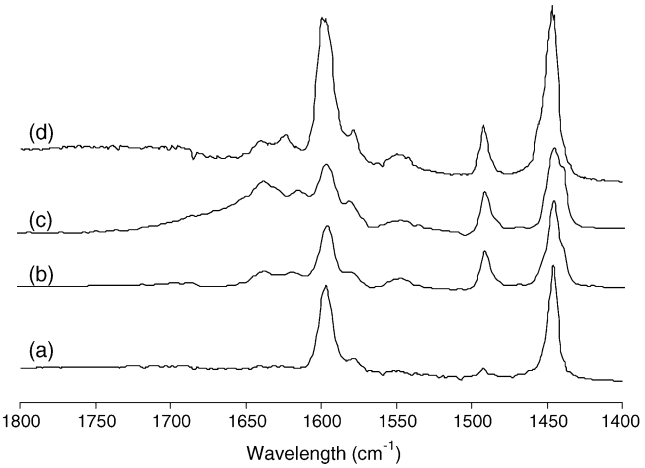

Fig. 5. IR pyridine adsorption at room temperature for (a) Al-MSU-S (Si/Al 70), (b) HY (Si/Al 60), (c) HY (Si/Al 10.4) and (d) Al-MCM-41 (Si/Al 70).

that of silica with the most intense bands in the range of 1440–1456 and 1560–1632 cm^{-1} and a very small band at ~1490 cm^{-1} (Fig. 5). Mesoporous Al-MCM-41 and microporous HY zeolites showed pyridine absorption bands characteristic of Brønsted and Lewis acidity.

3.3. Catalytic activity

Over the B_2O_3/SiO_2 catalysts, a plot of conversion versus time show a very fast initial rate followed by leveling of the conversion at times longer than 30 min to 1 h. The initial rate depended on the boron oxide loading and reached a maximum at 15 wt.% loading (Fig. 6). Despite the different activity, the selectivity towards campholenic aldehyde was independent of B_2O_3 loading. At room tem-

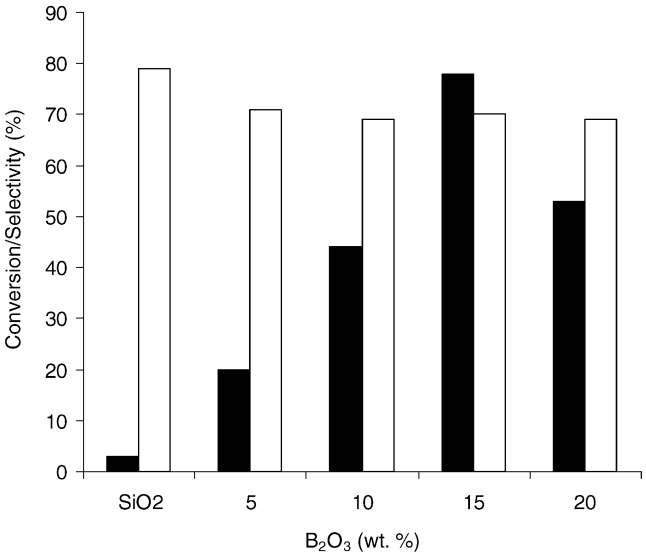

Fig. 6. Conversion (′) and selectivity (≤) to campholenic aldehyde over SiO_2 and B_2O_3/SiO_2 catalysts after 1 h at 25 °C.

Table 2
Comparison of conversion and selectivity over various catalysts for isomerisation of α-pinene oxide

Catalyst	Conversion[a] (%)	Selectivity[a] (%)
B_2O_3/SiO_2 (15 wt.%)	84	69
HY (Si/Al 10.4)	96	49
HY (Si/Al 24)	78	51
HY (Si/Al 60)	49	66
Al-MCM-41 (Si/Al 70)	65	53
$ZnCl_2$ (2 mmol g^{-1})	18	85
$ZnCl_2$ (4 mmol g^{-1})	23	73
$ZnCl_2$ (8 mmol g^{-1})	26	73
Al-MSU (Si/Al 70)	54	86

[a] After 4 h reaction at 25 °C.

perature, 25 °C, the selectivity was ∼69%. This is comparable to that observed over USY [1]. The side products observed include isomeric aldehyde (12.5%), *p*-cymene (4.1%), *iso*-pinocamphone (7.3%), *trans*-carveol (4%) and *trans*-sobrerol (2.1%). The slightly lower selectivity of B_2O_3/SiO_2 samples as compared to SiO_2 may be due to the presence of Brønsted acidity in the former. The framework rearrangement reactions leading to *trans*-carveol and *p*-cymene are indicative of Brønsted acidity.

With a higher loading of B_2O_3, more acidic sites are generated until the silica support is completely covered by the overlayer. From the catalytic results, it would appear that this happens at around 15 wt.% B_2O_3. Beyond this loading, Brønsted acidic sites due to the presence of boric acid predominate. The decrease of the reaction rate together with constant selectivity over the entire reaction time suggests that the catalytically active sites are deactivated. The catalysts recovered after the reaction had changed from white to a light yellow, indicating deposition of organic residues. Attempts to regenerate the catalyst by heat treatment at 350 °C in air for 8 h resulted in a brown material which had lower activity than the fresh catalyst.

By lowering the temperature to 0 °C, the selectivity to campholenic aldehyde could be increased to 71%. However, at 50 °C, a selectivity of 65% was measured, slightly lower than that at 25 °C. Irrespective of the reaction temperature, the same by-products were observed. From the temperature dependence, the activation energy for the isomerization reaction was calculated to be 30.6 kJ mol^{-1}.

A comparison of the B_2O_3/SiO_2 catalysts was made with other solid acids (Table 2). At 25 °C, Al-MCM-41 was almost as active as 15 wt.% B_2O_3/SiO_2 with a conversion of 65% after 4 h, but the selectivity to campholenic aldehyde was only 53%. The activity of microporous HY catalysts increased with increasing aluminium content. After 1 h at 25 °C, the conversion was between 33 and 66%, depending on the Si/Al ratio. The selectivity to campholenic aldehyde showed an opposite trend to conversion. After 4 h, the selectivity over HY (Si/Al 10.4) was only 49% while HY (Si/Al 60) had a selectivity of 66%. The other products over the HY zeolites were isomeric aldehyde (16%), *trans*-carveol (8%), isopinocamphone (6%), *p*-cymene (3%) and *trans*-sobrerol (3%). The higher amounts of *trans*-carveol, *p*-sobrerol and *p*-cymene formed may be explained by the higher Brønsted acidity of the HY zeolites as compared to B_2O_3/SiO_2 catalysts.

$ZnCl_2$ is used as a homogeneous catalyst for the isomerisation of α-pinene oxide. Heterogenisation was carried out by supporting the $ZnCl_2$ on MCM-41 to ensure a good dispersion of the Lewis acid sites. For loadings up to 8 mmol g^{-1}, the conversion at 25 °C was below 28% after 4 h. The activity increased with $ZnCl_2$ loading; the sample with 2 mmol g^{-1} $ZnCl_2$ was the least active but its selectivity to campholenic aldehyde was the highest, 85%, at 18% conversion. The selectivity is comparable to that reported for $ZnCl_2$ used as a homogeneous catalyst. However, samples with higher loading of $ZnCl_2$ had a selectivity of only 73% at conversions of 22–26%. In comparison, Al-MSU-S was surprisingly active for α-pinene oxide isomerisation. After 4 h reaction at 25 °C, the conversion was ∼54% with a high selectivity to campholenic aldehyde of 86%. While many other products besides campholenic aldehyde have been observed over acid catalysts, the number of isomers formed over the Al-MSU-S material was very much reduced. Only isomeric aldehyde and *iso*-pinocamphone were found along with campholenic aldehyde.

Both B_2O_3/SiO_2 and Al-MSU-S contained predominantly Lewis acidic sites and both types of catalysts are active for the isomerisation of α-pinene oxide. The excellent selectivity to campholenic aldehyde over Al-MSU-S catalysts with few side products may be due to the mixture of microporosity and mesoporosity inherent in these compounds as compared to B_2O_3/SiO_2 samples which are mesoporous. In Al-MSU-S samples, the mesoporous walls have microporous channels of zeolitic nature. Due to the thinness of the walls in Al-MSU-S, the diffusion length is short. Reaction can occur within the micropores but due to the short length of channels, the formed product can diffuse away from the active site before further reaction to other isomers occurs. The formation of the other isomers at longer reaction times indicates that subsequent isomerization of campholenic aldehyde occurs in a consecutive reaction.

4. Conclusion

B_2O_3/SiO_2 samples were catalytically active in the isomerisation of α-pinene oxide. The most active catalyst for the supported B_2O_3 samples was 15 wt.% B_2O_3/SiO_2. Irrespective of the B_2O_3 loading, the selectivity to campholenic aldehyde over these supported catalysts was around 69% when the reaction was conducted at 25 °C. Samples with 10 wt.% or higher B_2O_3 loadings had a mixture of Lewis and Brønsted acid sites. HY zeolites and Al-MCM-41 with both types of acidity also showed high conversions for α-pinene oxide isomerisation but the selectivity to campholenic aldehyde was <66% at 25 °C. The selectivity of HY zeolites was

higher with low aluminium content. In comparison, supporting $ZnCl_2$ on MCM-41 did not change the high selectivity of $ZnCl_2$ to campholenic aldehyde but its activity remained low. Al-MSU-S (Si/Al 70) was active with a high selectivity of 86% at 54% conversion. Pyridine IR studies revealed that the sample had predominantly Lewis acidic sites. The good activity and selectivity may be due to the presence of both micro- and mesopores inherent in its framework structure.

References

[1] W.F. Hölderich, J. Röseler, G. Heitmann, A.T. Liebens, Catal. Today 37 (1997) 353.
[2] K. Wilson, A. Rénson, J.H. Clark, Catal. Lett. 61 (1999) 51.
[3] P.J. Kunkeler, J.C. van der Waal, J. Bermmer, B.J. Zuurdeeg, R.S. Downing, H. van Bekkum, Catal. Lett. 53 (1998) 135.
[4] K.P. Peil, L.G. Galya, G. Marcelin, J. Catal. 115 (1989) 441.
[5] B.-Q. Xu, S.-B. Cheng, X. Zhang, Q.-M. Zhu, Catal. Today 63 (2000) 275.
[6] S. Sato, M. Kuroki, T. Sodesawa, F. Nozaki, G.E. Maciel, J. Mol. Catal. A 104 (1995) 171.
[7] Y. Liu, W. Zhang, T.J. Pinnavaia, J. Am. Chem. Soc. 122 (2000) 8791.
[8] Y. Liu, T.J. Pinnavaia, Angew. Chem. Int. Edit. 40 (2001) 1255.
[9] Y. Liu, T.J. Pinnavaia, J. Mater. Chem. 12 (2002) 3179.
[10] Z.T. Zhang, Y. Han, L. Zhu, R.W. Wang, Y. Yu, S.L. Qiu, D.Y. Zhao, F.S. Xiao, Angew. Chem. Int. Edit. 40 (2001) 1258.
[11] X. Hu, G.K. Chuah, S. Jaenicke, Appl. Catal. A 217 (2001) 1.
[12] L.Y. Chen, G.K. Chuah, S. Jaenicke, Microporous Mater. 12 (1997) 323.
[13] S.A. Bagshaw, S. Jaenicke, G.K. Chuah, Ind. Eng. Chem. Res. 42 (2003) 3989.
[14] H. Matsuhashi, K. Kato, K. Arata, Acid–base catalysis II, in: H. Hattori, M. Misono, Y. Ono (Eds.), Proceedings of the International Symposium on Acid–Base Catalysis II, Kodansha, Tokyo, 1994, p. 251.
[15] E.P. Parry, J. Catal. 2 (1963) 371.
[16] C.A. Emeis, J. Catal. 141 (1993) 347.